Low-Cost Tissue Oximetry Using Discrete Light-Emitting Diodes

Tuukka Panula, Inka Mustajoki, Katri Karhinoja, Maria Kjellman, Jukka-Pekka Sirkiä and Matti Kaisti

***Abstract*—Tissue oxygen saturation (StO_2) is an important biomarker used to monitor patients after a surgical intervention. StO_2 is often measured using various techniques that require expensive, bulky, and complicated instrumentation. We propose a low-cost instrument design to measure StO_2 level using discrete light-emitting diodes (LED) and a photodiode receiver. The instrument was tested using a liquid tissue phantom to verify the operation of the system *in vitro* during hemoglobin deoxygenation. A commercial spectrometer was used as a reference device. Furthermore, we tested the device *in vivo* by measuring skin StO_2 during a brachial artery occlusion test. The results of these experiments suggest that the device is capable of measuring StO_2 with sufficient accuracy and could provide a low-cost alternative to spectrometer-based tissue oximetry in clinical use.**

***Index Terms*—Tissue oxygen saturation, StO2, oximetry**

I. Introduction

Tissue oxygen saturation (StO_2) is commonly monitored after free tissue transfer surgery. Free tissue transfer is a reconstructive surgical procedure, where a healthy free flap is transferred to replace injured tissue area. The success of the procedure is highly dependent on the ability of the new flap to form microvascular connections with the surrounding site [1]. Revascularization in the tissue flap is often monitored for several days after the surgery, and in case of failure, early intervention allows the procedure to be repeated with a relatively high success rate [2]. This requires accurate and real-time instrumentation to monitor the tissue. Spectrometer-based solutions like T-Stat (Spectros Medical Devices Inc., USA) are popular in clinical use, but require costly instrumentation and specialized fiber optic probes [3]. In addition, tissue oxygen monitors using discrete light-emitting diodes (LEDs) and photodiodes have been reported before [4]. Near-infrared spectroscopy (NIRS) is a method widely used for measuring StO_2 in cerebral tissue [5]. While it uses LEDs and photodiodes, the spectral range is limited to 700-1000 nm. Additionally, The penetration depth of near-infrared light is fairly high, especially suitable for measuring the brain non-invasively.

We developed a low-cost tissue oxygenation sensor using discrete LEDs and a photodiode receiver. Unlike photoplethysmography, that measures the pulsatile flow of the blood, StO_2 measurement is based on the change in oxyhemoglobin (HbO_2) and deoxyhemoglobin (HHb) concentrations in the tissue. Since their respective absorption spectra are known, their concentration can be estimated from spectroscopic data. A minimum of two wavelengths is needed for StO_2 computation, but we selected six wavelengths in order to compare their response. The wavelengths were selected based on the distinguishable changes between the HbO_2/HHb spectra. The individual emission spectra of the LEDs were recorded using a spectrometer. The usability of discrete LED's to StO_2 analysis was not clear from the start. A major concern was the relatively wide emission spectra of the LEDs, which could prevent us from observing the expected change. Additionally, the overlapping spectra of different LEDs could affect the resolution of the measurement. We also took into account the different penetration depths of each wavelength. The higher wavelengths penetrate deeper into the tissue, thus probing different parts of the circulation (arteries). On the other hand, shorter wavelengths only penetrate deep enough to probe the arteriolar and capillary blood. A recent study revealed that the penetration depths (50% of the light passing) for 400 nm and 800 nm are approximately 0.09 nm and 1.4 mm, respectively. [6]

We validated the performance of the device using an *in vitro* tissue phantom and compared the deoxygenation response to that of a commercial spectrometer and by performing and analyzing *in vivo* brachial cuff occlusion measurements to induce a change in StO_2.

II. Materials and methods

A. Liquid phantom

Liquid phantom was prepared in order to have optical properties similar to that of human tissue. The solution consisted of 82% phosphate-buffered saline (PBS, 806552, Sigma-Aldrich, USA), 0.82% sodium-bicarbonate solution (SBS, S8761, Sigma-Aldrich, USA) for pH stabilization, 8.2% bovine blood (Veljekset Rönkä Oy, Finland) and 10% intralipid (20% IL, I141, Sigma-Alrdich, USA). The intralipid is a lipid emulsion comprising soybean oil and was used to modify the optical properties of the phantom to represent those of superficial tissue rather than blood. [3], [7], [8]

Deoxygenation of blood hemoglobin was achieved using dry yeast. 0.1 g of dry yeast and 0.5 g of table sugar were diluted into 50 ml of warm water (42°C). In some measurements 25 ml of warm water was used to speed up the deoxygenation reaction. [3], [7], [8] 1 ml of the yeast dilution was added to 15–25 ml blood solution. The mixture was then divided into two 50 ml polypropylene tubes (Sarstedt, Germany) – one

This project has received funding from the European Union's Horizon Europe research and innovation programme under grant agreement No 101115492. The work of Tuukka Panula was also supported by the Instrumentarium Science Foundation.

Panula, Mustajoki, Karhinoja, Kjellman, Sirkiä and Kaisti are with Department of Computing, Faculty of Technology, University of Turku, 20500 Turku, Finland tuukka.j.panula@utu.fi

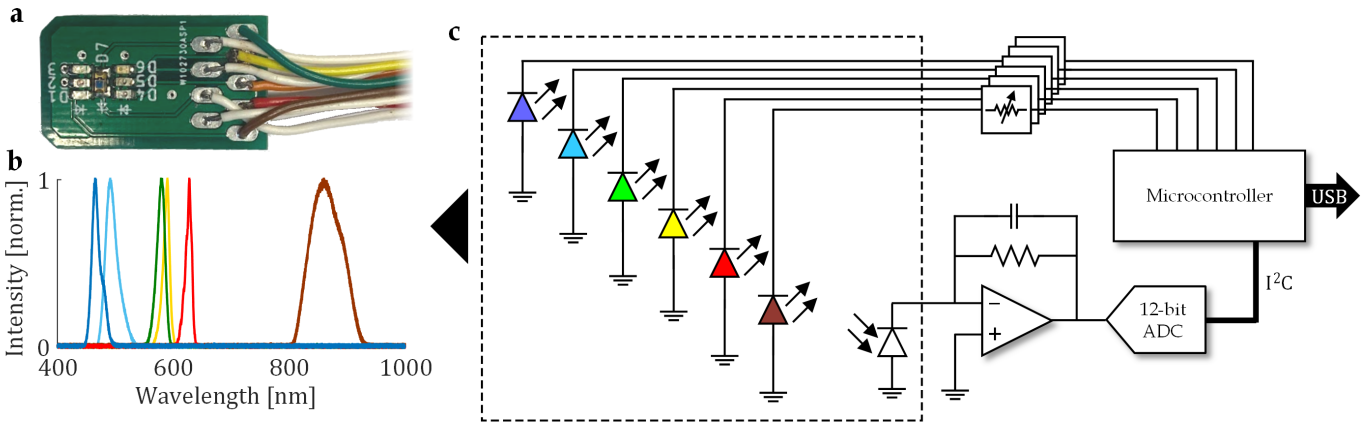

Fig. 1. a) A photograph of the probe PCB housing the six LEDs and the photodiode. b) Emission spectra of each LED measured using a commercial spectrometer. c) Hardware description of the proposed device. The highlighted area corresponds to the probe PCB shown in a).

for reference measurement using the spectrometer and another one for the developed device. The plastic tubes were placed into black solid 3D-printed enclosure to prevent external light from entering the solution. The parts were printed with Raise3D E2 (Raise 3D Technologies, USA) Fused Deposition Modeling (FDM) printer. Both probes were submerged in the solutions and held there for approximately 90 minutes. The tubes were sealed with Parafilm (Bemis Company, USA). The measurement was repeated three times. The setup is shown in Fig. 2a.

B. Spectrometer setup

The spectrometer reference comprised a FLAME-T-VIS-NIR-ES (Ocean Insight, USA) visible-to-near-infrared spectroscope, a tungsten halogen light source (HL-2000-HP, Ocean Insight) and a reflection/backscatter probe (QR400-7-VIS-BX, Ocean Insight). The spectrometer probe was covered with double-layer Parafilm to prevent direct contact between the liquid and the probe. The spectrometer was sampled at 0.2 Hz with exposure time of 3 ms. The spectral range was 345–1,041 nm with a pixel count of 3,648.

C. Electronics

A custom two-layer printed circuit board (PCB) was designed to house the LEDs (see Table I for details) and the photodiode (VEMD1060X01, Vishay Intertechnology, USA). ATmega328p (Microchip Technology, USA) was used as the microcontroller unit. The LED currents were set using six PTV09 potentiometers (Bourns Inc., USA). Each LED was pulsed individually with a pulse width of 10 ms. A transimpedance amplifier was constructed using a CA3140 BiMOS operation amplifier (Renesas Electronics, Japan) to convert the photodiode current to voltage. A 12-bit analog-to-digital converter ADS1015 was used to record the voltage. The sampling frequency was 13 Hz. The sensor PCB is shown in Fig. 1a.

TABLE I
SPECIFICATIONS FOR THE DISCRETE LEDS USED IN THE PROBE. THE WAVELENGTHS ARE REPORTED AS NOMINAL MANUFACTURER SPECIFIED VALUES AND MEASURED VALUES.

λ (nom.)	λ (meas.)	Model	Manufacturer
465 nm	465 nm	APHD1608LVBC/D	Kingbright
496 nm	491 nm	SMLD12E3N1WT86	ROHM
577 nm	579 nm	APHD1608LCGCK	Kingbright
590 nm	590 nm	APHD1608LSYCK	Kingbright
645 nm	628 nm	APHD1608LSURCK	Kingbright
880 nm	860 nm	APHD1608SF4CPRV	Kingbright

D. Algorithm and calibration

The optical densities (OD) for each wavelength were calculated with the following equation:

$$OD^{\lambda} = \log_{10}\left(\frac{I_0}{I}\right)^{\lambda} \quad (1)$$

where I_0 is the white reference value and I is the measured intensity at the desired wavelength λ. [7], [9], [10].

StO_2 was computed with the Knoefel algorithm [9]. Extinction coefficients ϵ were used for oxyhemoglobin and deoxyhemoglobin (HbO_2 and HHb respectively) and were adapted from [11]. The equations for computing the StO_2 are,

$$[HbO_2] = \frac{OD^{577}\cdot\epsilon^{555}_{deoxy} - OD^{555}\cdot\epsilon^{577}_{deoxy}}{\epsilon^{577}_{deoxy}\cdot\epsilon^{555}_{deoxy} - \epsilon^{555}_{deoxy}\cdot\epsilon^{577}_{deoxy}} \quad (2)$$

$$[HHb] = \frac{OD^{555} - [HbO_2]\cdot\epsilon^{555}_{oxy}}{\epsilon^{555}_{deoxy}} \quad (3)$$

$$[StO_2] = \frac{[HbO_2]}{[HbO_2]+[HHb]} \quad (4)$$

The raw values $StO_2^{DUT_{raw}}$ from our device were calibrated using the following method:

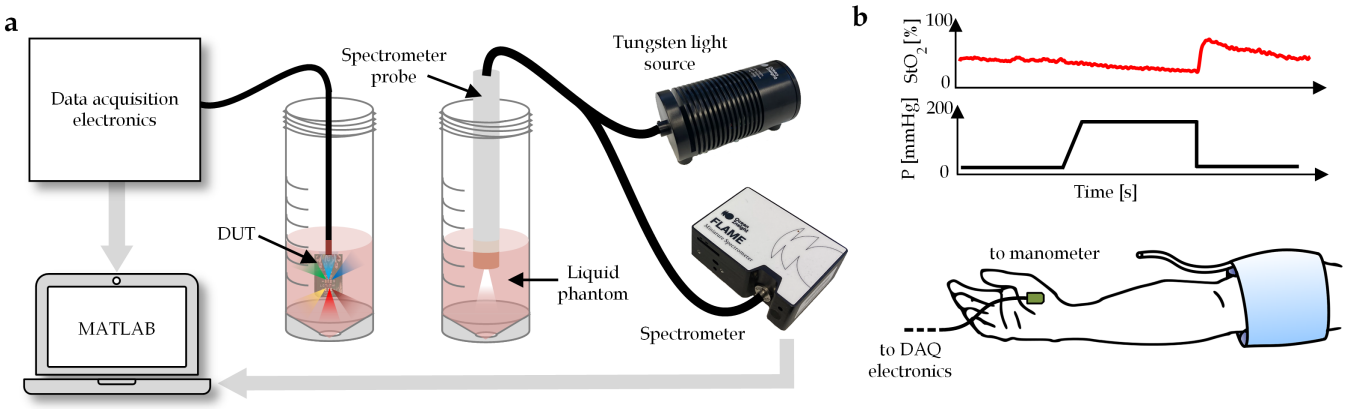

Fig. 2. Experimentation setup. a) To start the deoxygenation reaction, yeast was added to 25 ml of blood solution after which the solution was added to two 50 ml polypropylene tubes. Both devices were used to measure the reaction in the liquid phantom and the data from both were collected on a PC. b) Brachial occlusion test was done by inflating the cuff well above systolic pressure in order to seize the blood flow to the hand. Simultaneously, tissue oxygenation was measured using our device attached to the hand.

$$StO_2^{DUT_{cal}} = a + \frac{StO_2^{DUT_{raw}} - b}{c - b}(d - a) \qquad (5)$$

where a and d are the StO_2 values measured with the reference device from fully deoxygenated and oxygenated solutions respectively. Similarly, b and c are the StO_2 values measured with the our device from fully deoxygenated and oxygenated solutions respectively. The constants a - d were the same for all measurements.

E. Brachial cuff occlusion

For *in vivo* measurements we used a brachial occlusion test. This was done by inflating the cuff well above systolic pressure in order to seize the blood flow to the hand and simultaneously measuring the response with the developed StO_2 device. We took three measurements with our device using an aneroid sphygmomanometer (R1 Shock Proof, Rudolf Riester GmbH, Germany) as an occlusion cuff. First, a two-minute baseline was recorded, followed by a three-minute occlusion period, with the cuff pressure inflated to 200 mmHg. Finally, a two-minute recovery period was recorded after the cuff was released. The setup is shown in Fig. 2b.

III. Results

A. Measurement principle

We developed an optical sensor with discrete LEDs and a photodiode to measure StO_2. Instead of measuring the full spectrum, our device measures only six wavebands defined by the emission spectra of the discrete LEDs. Each of the LEDs is connected to GPIO pins of the microcontroller and pulsed in sequentially. The light from the LEDs is partly absorbed by the tissue, and the reflected light is measured with a photodiode at each LED duty cycle.

The LED wavelengths were selected to match certain points in the (deoxy)hemoglobin spectrum, allowing two pairs of LEDs with opposite response curves in regards to the de-oxygenation process to be used for StO_2 computation. For

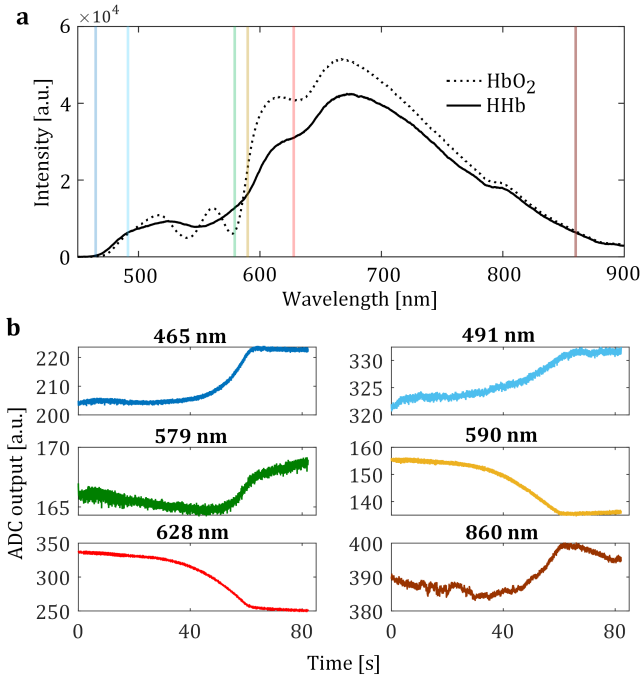

Fig. 3. a) Measured intensity at the beginning of an *in vitro* measurement when HbO_2 dominates and at the end when HHb dominates. The vertical lines illustrate the spectral peaks of the discrete LEDs. b) Changes in photodiode output for each discrete LED. The direction of the changes match the changes measured with the spectrometer at corresponding wavelenghts.

this study, we chose the 579 nm and 590 nm LEDs, since they probe the more superficial microvascular blood volume. These wavelengths were chosen because they correspond to the desired points in the HbO_2/HHb transition curve. The availability of LED with certain wavelengths was the reason we did not use the exact same wavelengths that were used for the reference device. As seen in Fig. 3b, the 579 nm signal increases as the deoxygenation proceeds, and the 590 nm signal decreases at the same time. We calculated OD^{579} and OD^{590} for both wavelengths using equation 1 and the white reference values.

B. Light source characterization

We measured the white reference signals I_0 with both the spectrometer and our device by measuring the response to white background. The measurement was done using the same light sources as in the *in vitro* tests. In addition, the spectrum of each LED was measured with the spectrometer. As seen in Fig. 1b, there is some overlap between the LED spectra, which is an inherent feature of the LED. This overlap can be a source of inaccuracy in the measurement. Overlap is observed between 466 nm and 491 nm as well as between 579 nm and 590 nm LEDs. Compared to the spectrometer, where the wavelengths can be selected freely and with high resolution, the width of the LED spectrum can result in incorporating both increasing and decreasing components of the HbO_2/HHb transition. The magnitude of these effects should be taken into consideration in a future study. Furthermore, for a commercial device, the variation in the manufacturer's frequency tolerances have to be taken into account.

C. In vitro deoxygenation measurements

Deoxygenation changes the absorption spectra of hemoglobin. Fig. 3a shows the difference in the absorption spectra of the oxygenated and deoxygenated tissue phantom at the beginning and the end of the measurement, respectively, measured with the commercial spectrometer. The changes in the absorption of the six wavelengths measured with our device are shown in Fig. 3b. The direction of the changes match the changes measured with the commercial spectrometer at the corresponding wavelengths. Fig. 4a shows a decrease in StO_2 in the tissue phantom measured with both our device and the commercial spectrometer. The variations between three measurements are shown in Fig. 4b. This depicted for both devices at the beginning (HbO_2 dominates) and at the end (HHb dominates) of the reaction. Mean and standard deviation (mean±SD) at the beginning and end of the measurement for the reference device were 67.5±0.4% and 6.1±0.2% respectively. For our device, the corresponding figures were 70.8±2.5% and 5.0±1.7%. The measurement starts with most of the hemoglobin in an oxygenated form and after 20 minutes it starts to decrease. Finally, at approximately 55 minutes, the decrease abruptly stops as all oxygen bound to the hemoglobin is used by the yeast. In our measurements, the measured values do not reach 100% and 0%, which is due to the algorithm used. In previous studies, the selection of the

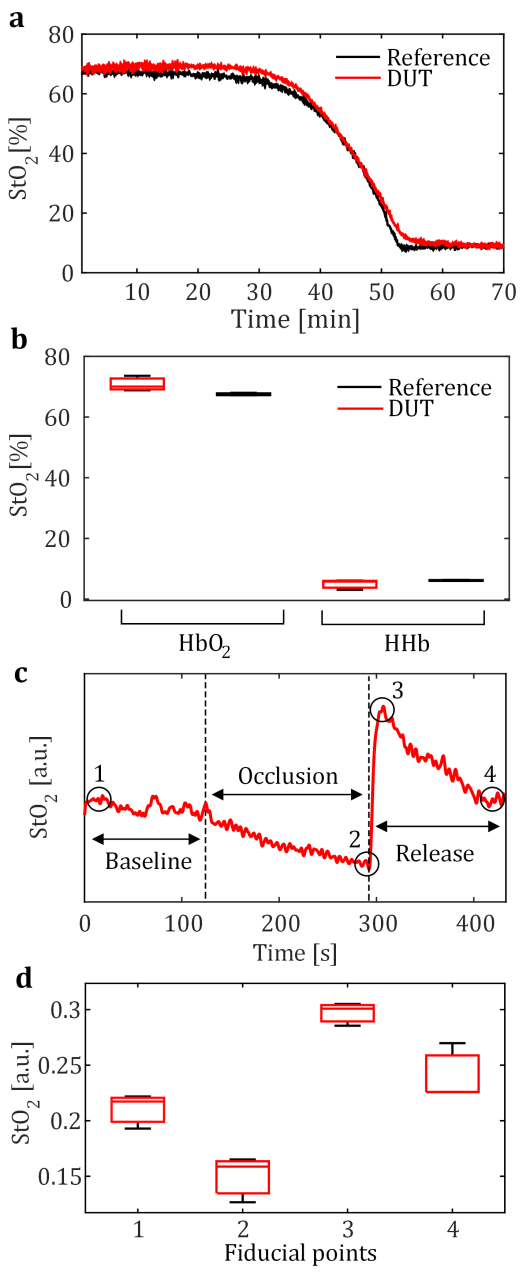

Fig. 4. a) Tissue phantom measurement done with the proposed device under test and the reference spectrometer. b) StO_2 levels at the beginning and end of the three measurements (With HbO_2 and HHb dominating respectively) shown in boxplots. c) Brachial cuff occlusion measurement done with the proposed device. Suprasystolic pressure was applied at 120 s and released at 290 s. Clear overshoot in StO_2 is visible after the cuff release. d) Variation between the three measurements at four distinct fiducial points highlighted in c) (1: baseline, 2: end of occlusion, 3: overshoot, 4: end of release).

algorithm has been shown to have an effect on the StO_2 value and results match the values reported in the literature [12]. A separate study comparing the algorithms on our device would be beneficial in the future. The ADC values recorded were fairly low in contrast with the ADC range. The photodiode signal gain was set low because the same setup was used to

measure the white reference, which resulted in much higher ADC counts and would have saturated the signal otherwise. Regardless, the signal quality was sufficient to measure the change in StO_2. We believe that in a real case measurement, a meaningful change in StO_2 could be measured with enough accuracy.

D. Brachial occlusion measurements

Brachial cuff occlusion is a standard method for assessing reactive hyperemia - a biomarker measuring the ability of the circulation to adapt to tissue hypoxia [13]. As seen in Fig. 4c, during the occlusion period, StO_2 decreases until the cuff is released. This is followed by a rapid increase or overshoot in StO_2. Finally, the saturation reverts to baseline. The box plots in Fig. 4d shows the variation between the three measurements at four distinct fiducial points (1: baseline, 2: end of occlusion, 3: overshoot, 4: end of release). We noticed that the tissue phantom values do not translate directly to occlusion measurement so we could not calibrate the results into actual StO_2 values. During cuff occlusion, the blood volume in the tissue is different compared to normal tissue perfusion, which can affect the reliability of the measurement. The occlusion measurements were only performed with our device, since the used spectrometer setup is not suitable for use in *in vivo* measurements.

IV. Conclusion

In this paper, we proposed a low-cost alternative to clinical-grade tissue spectrometer to measure tissue oxygenation level. This was achieved by choosing discrete LEDs with appropriate wavelengths for the measurement of (de)oxyhemoglobin. The operation of the design was verified using an *in vitro* liquid tissue phantom and by measuring tissue oxygenation *in vivo* from the skin during a brachial occlusion test.

The results show that the response at each wavelength follows the theoretical change, and the setup is, in fact, capable of measuring StO_2. In the future, an additional study is needed to calibrate the device for human tissue measurements, comparing it against a clinical grade tissue oximeter. We noticed that the *in vitro* calibration values do not directly translate to *in vivo* measurement values.

References

[1] Anthony D Dat, Ian W Loh, and Frank Bruscino-Raiola. Free-flap salvage: muscle only versus skin paddle–an australian experience. *ANZ journal of surgery*, 87(12):1040–1043, 2017.

[2] Allison A Slijepcevic, Gavin Young, Justin Shinn, Steven B Cannady, Matthew Hanasono, Matthew Old, Jeewanjot S Grewal, Tamer Ghanem, Yadranko Ducic, Joseph M Curry, et al. Success and outcomes following a second salvage attempt for free flap compromise in patients undergoing head and neck reconstruction. *JAMA Otolaryngology–Head & Neck Surgery*, 148(6):555–560, 2022.

[3] David A. Benaron, Ilian H. Parachikov, Wai-Fung Cheong, Shai Friedland, Joshua L. Duckworth, David M. Otten, Boris E. Rubinsky, Uwe B. Horchner, Eben L. Kermit, Frank W. Liu, Carl J. Levinson, Aileen L. Murphy, John W. Price, Yair Talmi, and James P. Weersing. Quantitative clinical nonpulsatile and localized visible light oximeter: design of the T-Stat tissue oximeter. page 355, San Jose, CA, July 2003.

[4] Melissa Berthelot, Francis Patrick Henry, Judith Hunter, Daniel Leff, Simon Wood, Navid Jallali, Elizabeth Dex, Ladislava Lysakova, Benny Lo, and Guang-Zhong Yang. Pervasive wearable device for free tissue transfer monitoring based on advanced data analysis: clinical study report. *Journal of Biomedical Optics*, 24(6):067001–067001, 2019.

[5] Hellmuth Obrig. Nirs in clinical neurology—a 'promising'tool? *Neuroimage*, 85:535–546, 2014.

[6] Louise Finlayson, Isla RM Barnard, Lewis McMillan, Sally H Ibbotson, C Tom A Brown, Ewan Eadie, and Kenneth Wood. Depth penetration of light into skin as a function of wavelength from 200 to 1000 nm. *Photochemistry and Photobiology*, 98(4):974–981, 2022.

[7] S. Kleiser, D. Ostojic, B. Andresen, N. Nasseri, H. Isler, F. Scholkmann, T. Karen, G. Greisen, and M. Wolf. Comparison of tissue oximeters on a liquid phantom with adjustable optical properties: an extension. *Biomedical Optics Express*, 9(1):86, January 2018.

[8] S. Kleiser, N. Nasseri, B. Andresen, G. Greisen, and M. Wolf. Comparison of tissue oximeters on a liquid phantom with adjustable optical properties. *Biomedical Optics Express*, 7(8):2973, August 2016.

[9] W. T. Knoefel, N. Kollias, D. W. Rattner, N. S. Nishioka, and A. L. Warshaw. Reflectance spectroscopy of pancreatic microcirculation. *Journal of Applied Physiology*, 80(1):116–123, January 1996.

[10] John Gade and Gorm Greisen. New porcine test-model reveals remarkable differences between algorithms for spectrophotometrical haemoglobin saturation measurements with VLS. *Physiological Measurement*, 37(9):1624–1635, September 2016.

[11] John Gade, Dorte Palmqvist, Peter Plomgård, and Gorm Greisen. Diffuse reflectance spectrophotometry with visible light: comparison of four different methods in a tissue phantom. *Physics in Medicine and Biology*, 51(1):121–136, January 2006.

[12] Nassim Nasseri, Stefan Kleiser, Ursula Wolf, and Martin Wolf. Tissue oximetry by diffusive reflective visible light spectroscopy: Comparison of algorithms and their robustness. *Journal of Biophotonics*, 11(9):e201700367, September 2018.

[13] Sébastien Lacroix, Mathieu Gayda, Vincent Gremeaux, Martin Juneau, Jean-Claude Tardif, and Anil Nigam. Reproducibility of near-infrared spectroscopy parameters measured during brachial artery occlusion and reactive hyperemia in healthy men. *Journal of biomedical optics*, 17(7):077010–077010, 2012.